Low temperature process to recover impaired waters

Veera Gnaneswar Gude[a]*, Nagamany Nirmalakhandan[a], Shuguang Deng[b]

[a]*Civil Engineering Department*, [b]*Chemical Engineering Department, New Mexico State University, Las Cruces, NM 88003, USA*
Tel. +1 (575) 646-3463; Fax +1 (575) 646-7706; email: john_us@nmsu.edu

ABSTRACT

A low temperature process based on physical principles of gravity and barometric head was developed for efficient recovery of potable water from impaired waters. An example of impaired water demonstrated in this study is secondary effluent from the local wastewater treatment plant. This paper illustrates two different configurations by which impaired waters could be processed; one using direct solar energy; and another using a low grade heat source. These configurations demonstrate the feasibility of utilizing renewable energy sources and waste process heat to drive the water recovery process making it an environment-friendly and cleaner approach. Experimental studies showed that the process was able to achieve the following reductions of key water quality parameters: total dissolved solids from 935 mg/L to 18 mg/L (>98%); total suspended solids from 5.1 mg/L to 0.15 mg/L (>97%); nitrates from 2.4 mg/L to < 0.1 mg/L (>95%); ammonia from 26.1 mg/L to < 0.5 mg/L (>98%); and coliform from 77 to ~0 mg/L (100%). The effect of process parameters such as heat source temperature, flow rate, and evaporation temperatures on the process performance is presented.

Keywords: Desalination; Water treatment; Wastewater; Effluent; Impaired waters; Low temperature process

1. Introduction

In many parts of the world, replenishment of natural potable water resources is exceeded by increasing demand for freshwater supply due to rapid industrialization and population growth. Desalination of brackish waters and seawaters is one of the current approaches for filling the shortfall between the demand for, and supply of freshwater. However, desalination by conventional technologies is both energy and cost intensive [1]. In lieu of desalination, which is possible only in some areas of the world where salt water (either brackish water or seawater) sources are readily available, recovery of potable-quality water from impaired sources can be considered for local reuse and recycling. Recovering potable water from impaired waters such as existing process effluents can be a feasible solution if the water recovery technology implemented is both energy and cost conservative and, if the energy required for the process is readily available in the form of waste heat and/or derived from a renewable source.

Water reuse is a well-accepted practice all over the world [2]. A potential impaired water source suitable for water recovery and reuse is wastewater generated locally [3–6]. However, wastewater treatment in many plants is limited to biological treatment (secondary treatment), while advanced or tertiary treatment is necessary before the recovered water could be considered for beneficial uses. Biologically treated wastewater can be a good candidate for water recovery because it does not require any pre-treatment and the salt concentration is considerably low as compared to other brackish water resources. As

---

* Corresponding author.

a result, the recovery of potable-quality water for non-potable uses from these impaired waters can be achieved at a cost much lower than that from typical brackish water sources. Even though many technologies are available for water recovery, some of them may not completely remove the coliform bacteria or require high dosage of chemical agents (ex: microfiltration, ultrafiltration and electrodialysis) [3, 7–9] and some need high quality mechanical energy with bio-fouling problems (e.g. reverse osmosis) [10]. The product from these technologies, in some cases, may not be suitable for surface or potable uses due to the presence of coliform bacteria and significant amounts of dissolved solids. Therefore, a process that provides superior treatment of impaired waters with the ability to utilize available low grade or renewable energy sources can be a better solution to produce potable-quality water in an economical and environment-friendly manner.

In this paper, two configurations of a low temperature water recovery process are presented which can be a low-energy and low-cost alternative for reclaiming high quality waters from impaired waters. The process operates under near-vacuum pressures and at low temperatures utilizing low grade heat sources such as waste heat releases or renewable energy sources such as solar energy [11–14]. Since the process operates at low temperatures, low cost construction materials can be used in fabricating the unit with minimal scaling problems [15]. Feasibility of this low temperature water recovery process to recover potable water from brackish water sources and secondary effluent of a local wastewater treatment plant is demonstrated in this study. Two different heat sources — direct solar energy and a low grade thermal source were used to drive the proposed process in these tests. Results from experimental studies, product water quality analysis and possibility of connecting the process to an available energy source in the local wastewater treatment plant are presented.

1.1. Proposed process configuration

The premise of the proposed approach can be illustrated by considering two barometric columns at ambient temperature, one with freshwater and one with feed water as shown in Fig. 1. The barometric columns contain the head equivalent to local atmospheric pressure and when closed, a vacuum will be created in the headspace by the amount of the fluid volume displaced by gravity. Due to the natural vacuum generated by this process, the head space of these two columns will be occupied by the vapors of the respective fluids at their respective vapor pressures. If the two head spaces are connected to one another, water vapor will distill spontaneously from the freshwater column into the feed water column because, the vapor pressure of freshwater is slightly higher than that of feed water at ambient temperature (Fig. 1a). However, if the temperature of the feed water column is maintained slightly higher than that of the fresh water column to raise the vapor pressure of the feed water side above that of the fresh water side, water vapor from the feed water column will distill into the fresh water column (Fig. 1b). A temperature differential of about 10–15°C is adequate to overcome the vapor pressure differential to drive this water recovery process. Such low temperature differentials can be achieved using low grade heat sources such as solar energy, waste process heat, thermal energy storage systems, etc.

A schematic arrangement of the low temperature water recovery system based on the above principles is shown in Fig. 2a. Components of this unit include an evaporation chamber (EC), a natural draft condenser, heat exchanger, and three barometric columns. These three columns serve as the feed water column; the waste withdrawal column; and the freshwater column, each with its own constant-level holding tank. These holding tanks are installed at ground level while the EC is installed

a) Freshwater and impaired water columns at 25°C

c) Freshwater column at 25°C and impaired water column at 45°C
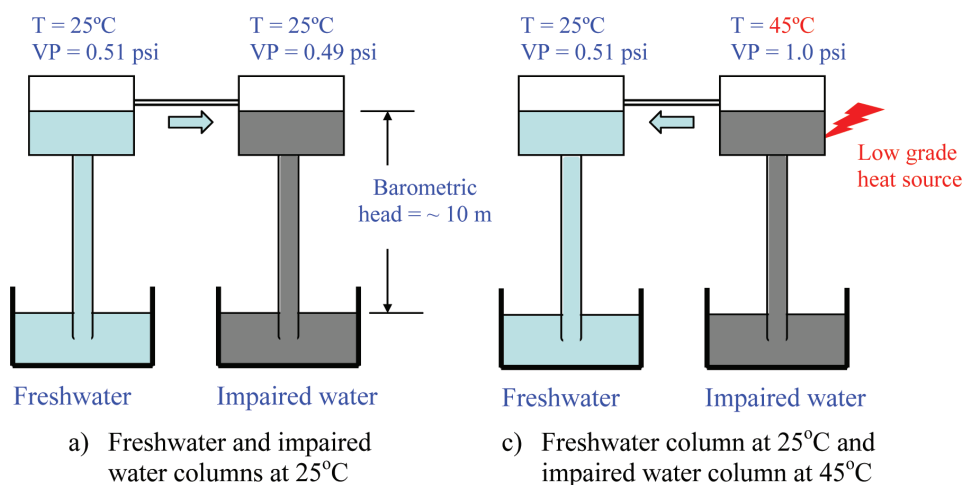
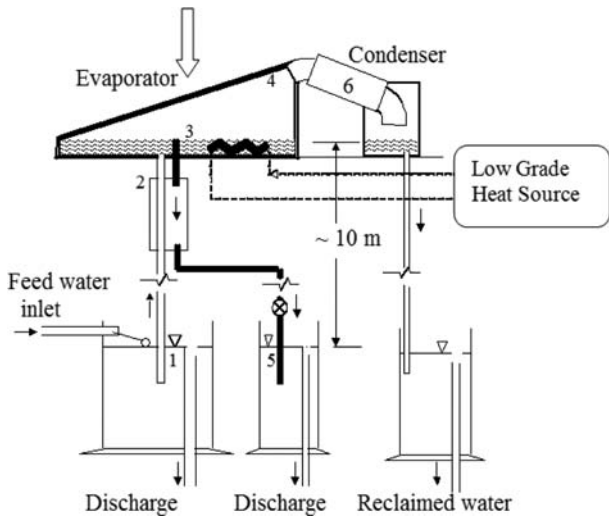Fig. 1. Low temperature water recovery process.

Fig. 2a. Schematic of process configuration.

atop the feed water and waste withdrawal columns at the barometric height of about 10 m above the free surface in the holding tanks to create a Torricelli's vacuum in the head space of the EC. The top of the freshwater column is connected to the outlet of the condenser. When the temperature of the feed water in the EC is increased by about 10–15°C above ambient temperature, water vapor will flow from the evaporator to the condenser where it will condense and flow into the freshwater column. By maintaining constant levels in the holding tanks with suitable withdrawal rates of waste and recovered water, this

configuration enables the water recovery process to be run without any mechanical energy input for fluid transfer or holding the vacuum [11,13]. However, a vacuum pump may be necessary to remove the accumulated non-condensable gases intermittently to maintain the natural vacuum in the evaporation chamber [11]. If a vacuum leak occurs, the system will fail to function and cross contamination may occur. The leaks in the system should be rectified before restarting the unit. The purpose of the heat exchanger is to preheat the feed water by the waste stream withdrawn from the evaporation chamber. Fig. 2b illustrates the process on a pressure-enthalpy diagram.

1.2. Theoretical analysis of the proposed process

Mass and heat balances around the evaporation chamber (EC) yield the following coupled differential equations, where the subscripts refer to the state points shown in Fig. 2a. The variables are defined in the Appendix.

Mass balance on volume of water in EC:

$$\frac{d}{dt}(\rho V)_{EC} = m_2 - m_5 - m_3 \qquad (1)$$

Mass balance on solute or contaminant in EC:

$$\frac{d}{dt}(\rho V C)_{EC} = m_2 C_2 - m_5 C_5 \qquad (2)$$

Heat balance for volume of water in EC:

$$\frac{d}{dt}(\rho V c_p T)_{EC} = Q_{in} + (m c_p T)_2 - (m c_p T)_5 - m_3 h_{L(T)} - Q_l \qquad (3)$$
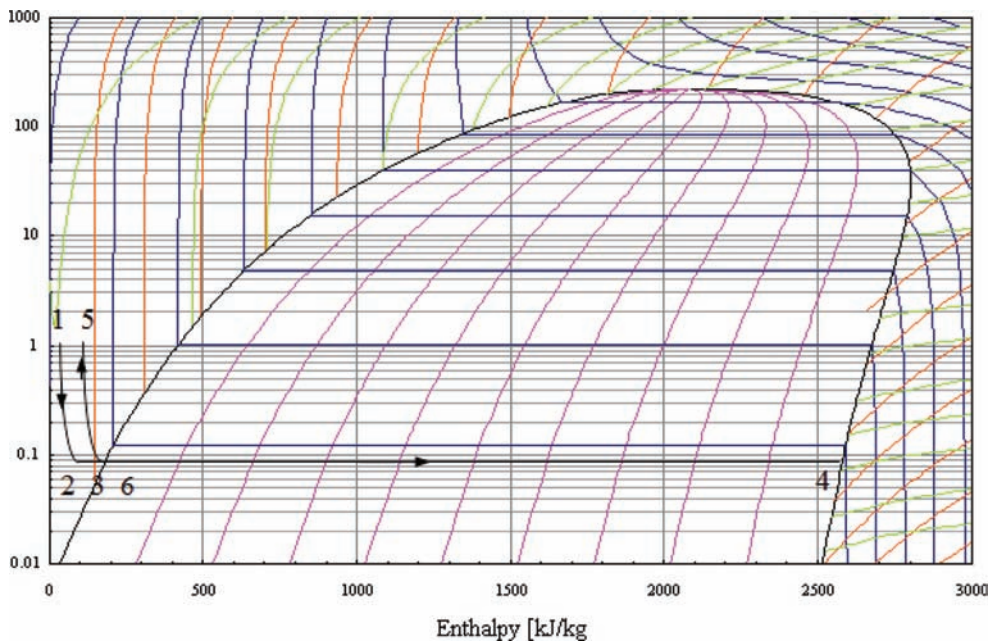

Fig.2b. Process illustrated in pressure-enthalpy diagram. State points relate to Fig. 2a.

where Q_{in} is the rate of heat input to the EC and Q_l is the rate of heat loss from the EC.

In this work two different heat sources are considered. In Configuration A, the heat input is via direct solar insolation on the EC and in Configuration B, a low grade thermal source around 60°C has been considered.

The heat input rate to the EC in Configuration A is expressed as:

$$Q_{in} = I_{(t)} A_{SEC} \alpha_w \tau_g \tag{4}$$

The heat input rate to the EC in Configuration B is expressed as:

$$Q_{in} = m_h C_{ph} (\Delta T) \tag{5}$$

Water recovery efficiency is defined as

$$\eta = \frac{M h_{L(T)}}{\Sigma (Q_{in} \Delta t)} \tag{6}$$

where latent heat can be calculated by [12]

$$h_{L(T)} = 3,146 - 2.36 (T + 273) \tag{7}$$

Evaporation rate as a function of pressure and temperature is expressed as [12]:

$$m_3 = A_{EC} \kappa \left[f_{(C_{EC})} \frac{p_{(T_3)}}{(T_3 + 273)^{0.5}} - \frac{p_{(T_6)}}{(T_6 + 273)^{0.5}} \right] \tag{8}$$

where

$$\begin{aligned} p_{(T)} = \big[&\exp(63.02 - 7139.6 / (T + 273) \\ &- 6.2558 \ln(T + 273) \big] \times 10^2 \, \text{Pa} \end{aligned} \tag{9}$$

The above equations are solved using Extend (Imagine That Inc., San Jose, CA) simulation software. Details of heat transfer relations for evaporation chamber and condensation surface, and heat losses by convection and radiation are presented elsewhere [16].

2. Experimental setup

Experimental studies were conducted with two different process unit designs and heat sources. The first is similar to the design shown in Fig. 2a with separate evaporation and condensation chambers (Configuration A), while in the second design, the evaporator and condenser unit are integrated with the condensing surface attached to the top of the evaporation chamber (Configuration B). The rationale for Configuration B is to reduce the foot print of the process unit thereby decreasing the capital cost and simplifying the process operation. Configuration A was tested with direct solar energy as a heat source while Configuration B was tested with a low grade thermal source, a hot water tank in this study. Prototype version of the test system is shown in Fig. 3.

Fig. 3. Prototype system.

2.1. Configuration A

An evaporation area of 0.2 m^2 and a condenser area of 0.2 m^2 were used in experimental studies. The results obtained from the experimental studies are used to extrapolate the performance of the process unit for 1 m^2 area of evaporation chamber. The evaporation chamber was fitted with a transparent Plexi-glass top to allow solar insolation for evaporation of freshwater. Feed water sources tested in this configuration were synthetic brackish water (Configuration A1) and secondary effluent from the local wastewater treatment plant (Configuration A2).

2.2. Configuration B

The experimental system consisted of 0.2 m^2 evaporator area and 0.22 m^2 condenser cover area. The evaporator was made of steel of thickness 0.635 cm and the condenser cover was made up of 0.5 cm thick aluminum. A hot water tank served as a low grade heat source; hot water was circulated through the evaporation chamber via a heat exchanger. Secondary effluent from the local wastewater treatment plant was tested as source water in these tests. The condenser cover was designed to reject heat to the

atmosphere or to a cooling water flow (500 mL/h of cold water at 30°C); system performance was tested under these two methods of heat rejection.

The process parameters were automatically measured and recorded in the data logger at 10-min intervals. Ambient temperature was measured by a thermocouple with an accuracy of ±0.2%; evaporation chamber temperature by a thermocouple with an accuracy of ±0.2% and the evaporation chamber pressure and condenser pressure by pressure transducers with an accuracy of ±0.3%. Experiments were conducted at different evaporation chamber temperatures. The depth of water in the evaporation chamber was fixed at 0.05 m. A rain gauge sensor with an accuracy of ±1% was used to measure freshwater production rate.

Thermocouples and pressure transducers were calibrated using a standard calibration procedure to establish their accuracy. Thermocouples were calibrated with two temperature points; the boiling point and freezing points of water, $T_h = 100°C$ and $T_l = 0°C$ respectively. Average values of 200 readings in 10 s period were taken for each of the temperature values. A linear response relationship was assumed for temperature change in the range 0–100°C and actual measured temperatures were calculated. Similarly, for pressure transducers, total of 200 readings were taken in the vacuum range 0–14.7 psi and a linear relationship was used to calibrate in the pressure range measured. Error analysis was performed for three different sets of readings recorded; an arithmetic mean, standard deviation and standard error were calculated.

3. Results and discussion

3.1. Configuration A

3.1.1. Configuration A1: Using direct solar energy with synthetic brackish water

Initially, Configuration A was simulated with the following parameters: solar energy incident on evaporation chamber (SEC) area of 1 m²; water depth in the EC of 0.05 m; and the reference temperature of 25°C. These simulation studies showed that, Configuration A could produce up to 5.25 L/d of freshwater, about 150% more than the productivity of a flat basin solar still which produce about 3–4 kg/d-m² [11]. This advantage over the solar still is due to the lower evaporation temperature where by significant energy need for the sensible heat has been averted. Thermal efficiencies of 60–70% could be achieved by this configuration.

Based on simulation results, an experimental prototype system was developed with an evaporation chamber area of 0.2 m². Synthetic brackish water was provided as a feed source. Since the evaporation rate at given temperatures and pressures is a factor of area as expressed in Eq. (8), the experimental results from this system were extrapolated to evaporation area of 1 m² to enable com-
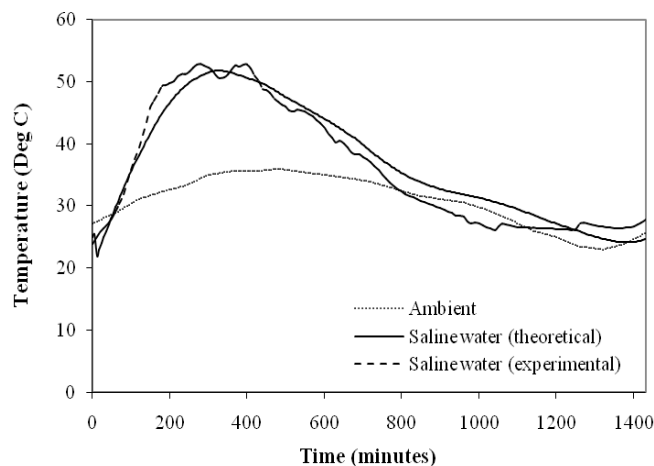

Fig. 4. Typical temperature profiles in Configuration A over 1-d period.

parisons between the experimental results and theoretical simulations. Experimental data from a typical run starting from a "cold start" are shown here to demonstrate the adequacy of the model presented earlier.

Fig. 4 compares the temperature of the EC predicted by the model against the measured temperature and the ambient temperature in Configuration A. During this test, the solar insolation reached a peak of 1,150 kJ/h-m² over the 8-h photoperiod. The maximum ambient temperature recorded was 36°C and the maximum temperature of the EC recorded was 52.75°C, while the predicted maximum temperature was 52°C. As shown in Fig. 4, EC temperature declined after the sunlight period, and approached ambient temperature after sunset. The correlation between the predicted and measured EC temperature was satisfactory with $r^2 = 0.943$, $F = 2358.2$, $p < 0.001$.

The predicted distillate volume during the above test is compared against the measured distillate volume in Fig. 5. Cumulative volume predicted by the model for a 24-h period was 5.25 L/d-m² while the measured value was 4.95 L/d-m². The difference (of 5.5%) in the cumulative distillate volume is mainly due to the assumption that the entire volume of the vapor distilled on the freshwater side whereas, during the test it was observed that some of the vapor condensed on the roof of the evaporator and trickled back to the evaporation chamber. Correlation between the predicted and measured distillate volume as a function of time was strong with $r^2 = 0.988$, $F = 11,839.4$, $p < 0.001$. The process efficiency as a function of time predicted by the model is compared in Fig. 6 against the efficiency calculated using the measured distillate volume from Eq. (5). The predicted efficiency averaged 64% while the observed efficiency averaged 61% over this test period. Correlation between the predicted and measured efficiency was strong with $r^2 = 0.985$, $F = 538.7$, $p < 0.001$.
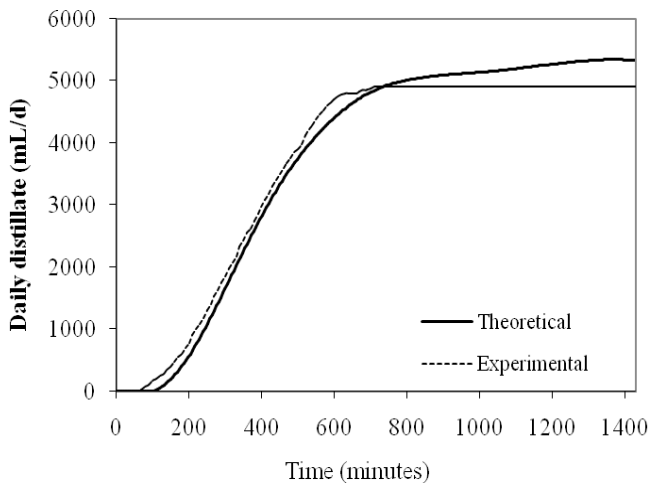
Fig. 5. Daily distillate production in configuration A: measured vs. predicted.
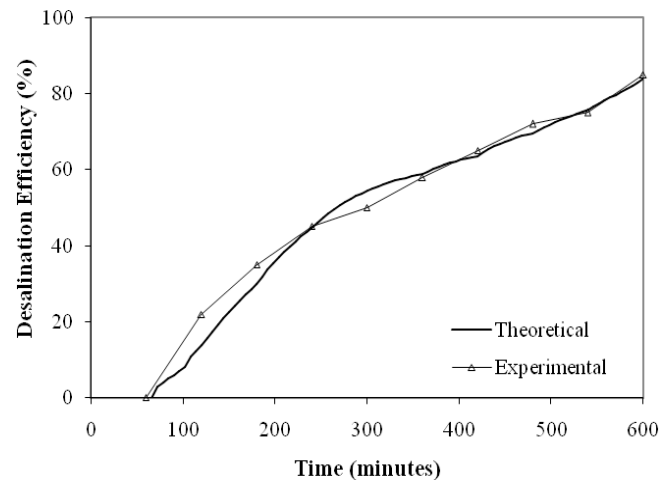

Fig. 6. Desalination efficiency in Configuration A: measured vs. predicted.

3.1.2. Configuration A2: Using direct solar energy with secondary effluent

In these tests, secondary effluent was used as a feed source in Configuration A1. The water quality test results for the feed and products are presented in Table 1.

The experimental results confirmed that the process can be operated at near vacuum pressures to maintain the flow of fluids without any mechanical energy input. The feasibility of using direct solar energy for recovering potable quality water was demonstrated by the above results. The distillate output from this unit is nearly twice that can be obtained from a simple solar still based on similar solar insolation values. This configuration is best suited for domestic applications with low requirements of non-potable water. However, higher rates of potable water recovery are possible with scale up of process design using solar energy. In other words, increasing the

evaporation area will result in higher freshwater output. Furthermore, this process can be engineered to utilize low grade waste heat released from other domestic process appliances such as heat rejected from air-conditioning systems or diesel generators. In a previous study, the use of heat rejected by an absorption refrigeration system (ARS) in driving this process has been simulated [17,18]. In that study, it was shown that the heat rejected by an ARS of cooling capacity of 3.25 kW (0.975 tons of refrigeration) along with an additional energy input of 208 kJ/kg of desalinated water was adequate to produce potable-quality water at an average rate of 4.5 kg/h.

3.2. Configuration B: Using low grade heat source with secondary effluent

A low grade thermal source (a hot water tank), was used as heat source in these tests. During these tests, the

Table 1
Characteristics of secondary effluent and product water

Parameter	Configuration A using solar energy			Configuration B using low grade heat			USEPA drinking water standard
	Secondary effluent	Recovered water	% Reduction	Secondary effluent	Recovered water	% Reduction	
BOD, mg/L	15.2	—	—	12.7	—	—	—
TDS, mg/L	935	18	98.1	783	16	98	500
TSS, mg/L	5.1	0.4	92.6	8	0.3	96.2	—
Nitrate as N-mg/L	2.4	<0.1	95.8	2.6	<0.1	96.2	10
Nitrites as Nmg/L	2.4	<0.1	95.8	2.6	<0.1	96.2	1
NH3 as N-mg/L	26.1	0.5	98.1	22.7	1.57	93.1	—
Chlorides, mg/L	0	0	—	0.5	0	100	4
Coliform, cfu	77	0	100	110	0	100	0
pH	7.1	7.0	—	7.6	7.6	—	6.5–8.5

circulation rate of the hot water was maintained at 9 kg/h while the temperature of the source was varied between 50–70°C. Typical temperature profiles recorded during continuous operation mode are presented in Fig. 7. The operating temperatures and pressures increased with the heat source temperature as shown in Fig. 8. Results from these tests showed that the low temperature water recovery system operated with higher efficiency at lower evaporation temperatures since the losses to the ambient are reduced (Figs. 9 and 10). At higher evaporation temperatures, the heat dissipation rate depends on the condenser surface area available and thus mass of water evaporated. Hourly freshwater production rates ranged 77–91 ml/h. Thermal energy supplied through the hot water source for temperature range 50–70°C varied between 355 and 395 W while thermal efficiency declined from 53% to 47%.

The effect of heat source flow rate was studied in the range of 9–16 kg/h. Thermal efficiency decreased with increasing heat source flow rate as shown in Fig. 11. This is because the condenser cover can only dissipate certain amount of latent heat to the environment which is limited by the condenser cover area. Higher flow rate will result in high vapor flow rates initially increasing pressure in the evaporator thus reducing the yield rate. A reasonable flow rate has to be considered for better yield rate. It is suggested that the flow rate should match the energy dissipation rate of the condenser cover or lower efficiencies will result. In this study a reasonable yield rate was obtained with a heat source flow of 9 kg/h at different heat source temperatures.

The yield rate can be increased by cooling the condenser with recycle water or source water. Cooling had significant effect on the efficiency as shown in Fig. 12. A small flow of 500 ml/h of freshwater was allowed to flow on the condenser cover which was collected at the bottom of the condenser. Fig. 12 shows that an increase in thermal efficiency of 10–15% can be achieved with cool-
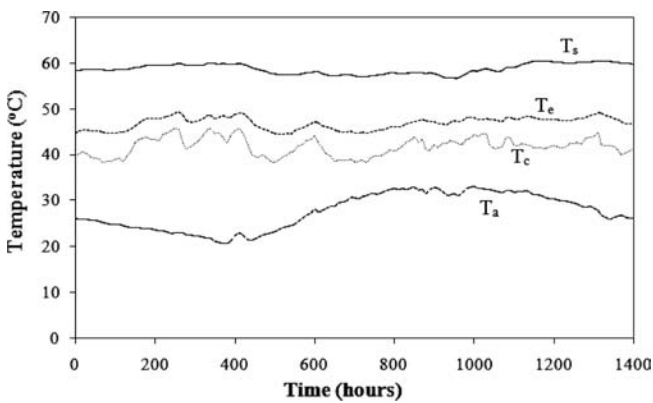

Fig. 7. Temperature profiles of the low temperature water recovery process (T_a = ambient temperature, T_c = condenser cover temperature, T_e = impaired water temperature, T_s = heat source temperature).
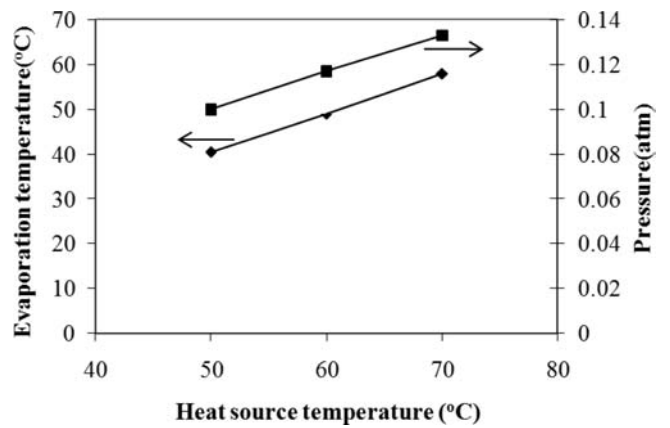

Fig. 8. Operating temperatures and pressures for different heat source temperatures.
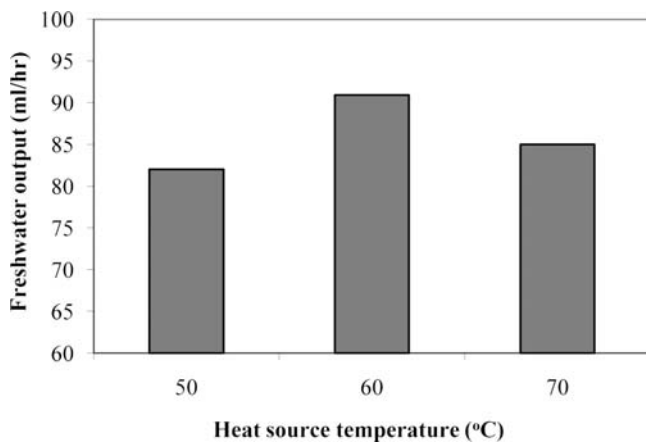

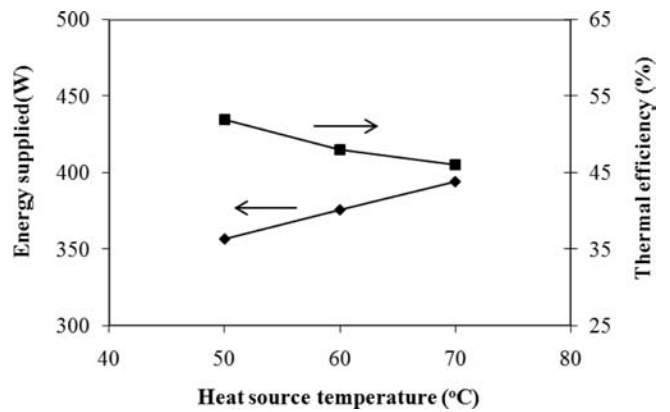Fig. 9. Freshwater production rate with heat source temperature.

Fig. 10. Energy supply and efficiency for different heat source temperatures.
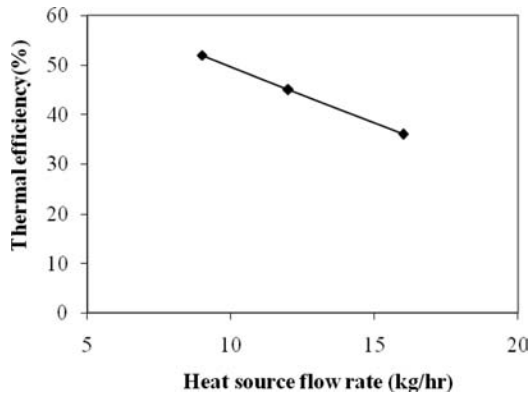
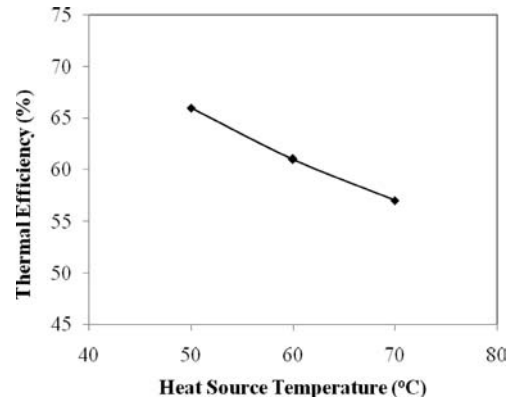Fig. 11. Effect of heat source flow rate on thermal efficiency.

Fig. 12. Effect of cooling on thermal efficiency.

ing. Thermal efficiency increased from a maximum value of 53–67% for heat source temperature at 50°C (Fig. 12).

The efficiency can be improved further with adequate insulation between the evaporator basin and condenser top, addition of fins on the condenser plate for more efficient heat dissipation and external cooling by recycling the product water. This configuration can be scaled to large scale applications depending on the availability of suitable low grade heat sources. As an illustration, a case study for the City of Las Cruces wastewater treatment plant is described below.

3.2.1. Case study

The City of Las Cruces wastewater treatment plant treating an average of 10 MGD of wastewater has anaerobic sludge digester in place to process the biomass. The anaerobic digester produces biogas which can generate up to 350 kW of energy on a daily basis [19]. Based on the

model simulations, a multi-effect low temperature unit demonstrated in this study with a gain to output ratio (GOR) = 5 would require a specific energy consumption of 470 kJ/kg of potable-quality water produced. A total volume of 17000 gal/d of freshwater can be produced from the plant effluent by utilizing the energy generated by the biogas. This freshwater can be used for process cooling operations, plant maintenance, or cooling and heating applications saving the water and heating bills for the wastewater treatment plant or can be sold to other industrial or irrigation applications.

3.2.2. Cost analysis

Economic analysis was performed for the low temperature desalination system and compared with a solar still. Detail cost estimates are shown in Table 2. A daily freshwater production of 3 L/d and 5 L/d were assumed for solar still and low temperature process respectively.

Table 2
Cost comparison for low temperature process and solar still

Item	Description	Estimated cost (US$)	
		Low temperature process	Solar still
Evaporator	1 m² cross sectional area	250	200
Evaporator heat exchanger	1.27 cm copper tube, 5 m long	30	
Condenser		150	50
Tube-in-tube heat exchanger	1.27 cm inside copper tube, 2.54 cm outside PVC tube	25	
PVC pipes	PVC tube of 1.27 cm diameter and 30 m long	30	
Pipe fittings		20	
Storage tanks	Four, 20 L capacity	60	15
Supporting structure	32 ft high structure (existing structure)		
Labor		120	60
Miscellaneous		50	50
Total cost		735	375

Freshwater production costs were determined based on the assumption that the investment is financed at an annual interest rate of 5% over the lifetime of 15 years for both the systems [20]. The unit production cost for low temperature process, $0.039/L was comparable to the unit product cost for solar still, $0.033/L. The low temperature process has certain advantages such as higher energy efficiency and higher fresh water production rates with addition of external heat source for a given unit size.

3.3. Water quality

The source water contained biochemical oxygen demand (BOD), dissolved solids (TDS), suspended solids (TSS), nitrates, nitrites, chlorides and coliform bacteria. However, the process was able to achieve more than 90% reductions for each of the above contaminants. Fecal coliform was measured by membrane filter technique, USEPA approved test procedure #9222 D by American Public Health Association, APHA [21]. In case of microbial residuals, it is necessary to perform disinfection as an additional level of protection before non-potable uses. The process produces high quality distillate with TDS < 50 ppm which is suitable for many non-potable uses. Feed water characteristics and recovered potable water characteristics are summarized in Table 1 for both configurations A and B. The water characteristics were tested and reported by Interlab and SWAT laboratories on the NMSU campus.

4. Conclusions

A process capable of utilizing low grade heat sources such as direct solar energy or process waste heat to produce high quality potable water from impaired waters is proposed. Two alternate configurations for implementing the proposed process were investigated at prototype scale. This study demonstrated the feasibility of these two configurations in recovering potable water from effluents from wastewater treatment plants and brackish waters. Experimental results confirmed that the process was able to achieve more than 95% reductions of total dissolved solids; total suspended solids; nitrates; ammonia; and coliform bacteria. This study demonstrated that the proposed configurations do not consume any non-renewable energy sources or generate any environmental emissions in reclaiming high quality water from impaired sources. As such, it can potentially be an environmental-friendly approach compared to current fossil-fuel dependent technologies.

Acknowledgement

Symbols

A	—	Surface area, area of evaporation chamber, m^2
C	—	Concentration of solute, kg/kg
c_p	—	Specific heat, kJ/kg-K
$f_{(c)}$	—	Concentration correction factor
h	—	Heat loss coefficient
$h_{L(T)}$	—	Latent heat at temperature T, kJ/kg
I	—	Solar insolation, kJ/h-m^2
M	—	Total daily mass of distillate, kg
m	—	Mass flow rate, kg/h
Q	—	Heat flow rate, kJ/h
T	—	Temperature, °C
U	—	Heat transfer coefficient, kJ/m^2-h-oC
V	—	Volume, m^3

Greek

α	—	Absorptivity
ε_w	—	Emissivity of saline water
η	—	Efficiency
κ	—	Experimental constant, 10^{-7}–10^{-6} kg-m^{-2}-Pa^{-1}-s^{-1}-K$^{0.5}$
ρ	—	Mass density, kg/m^3
τ	—	Transmissivity

Subscripts

a	—	Ambient
co	—	Condenser
EC	—	Evaporation chamber
g	—	Glass
h	—	Hot water
l	—	Losses
PV	—	Photovoltaic panel
w	—	Water

References

[1] T. Pettersen, A. Argo, R.D. Noble and C.A. Koval. Design of combined membrane and distillation processes. Separ. Technol., 6 (1996) 175–187.

[2] US EPA, Guidelines for Water Reuse. US Environmental Protection Agency, Report No.EPA/625/R-04/108, 445, 2004.

[3] E. Ortega and R. Iglesias, Reuse of treated municipal wastewater effluents in Spain: Regulations and most common technologies, including extensive treatments, Desal. Wat. Treat., 4 (2009) 148–160.

[4] K. Madwar and H.Tarazi, Desalination techniques for industrial wastewater reuse, Desalination, 152 (2002) 325–332.

[5] H. Kon and M. Watanabe, Construction of a treated wastewater reuse system for renewal of a water cycle mechanism in urban areas — Modeling analysis of reclamation treatment processes corresponding to target water quality by use, Desal. Wat. Treat., 6 (2009) 5–11.

[6] E.P. de la Parte, Desalination and reclaimed water - Emerging issues in Eastern Water Law; 15th Annual Section Fall Meeting, Pittsburgh, PA, September 26–29, 2007.

[7] M.P. del Pinoa and B. Durham, Wastewater reuse through dual-membrane processes: Opportunities for sustainable water resources, Desalination, 124 (1999) 271–277.

[8] J.T. Aguinaldo, Application of integrated chemical precipitation and ultrafiltration as pre-treatment in seawater desalination, Desal. Wat. Treat., 2 (2009) 113–125.

[9] S.A.A. Tabatabai, M.D. Kennedy, G.L. Amy and J.C. Schippers, Optimizing inline coagulation to reduce chemical consumption in MF/UF systems, Desal. Wat. Treat., 6 (2009) 94–101.

[10] T.H. Kim, Y.S. Kim, Y.H. Choi, J.H. Kweon, J.H. Song and N.W. Gang, Biofilm formation and its effect on biofouling in RO membrane processes for wastewater reuse, Desal. Wat. Treat., 2 (2009) 70–74.

[11] S. Al-Kharabsheh and D.Y. Goswami, Analysis of an innovative water desalination system using low-grade solar heat, Desalination, 156 (2003) 323–332.

[12] A. Midilli and T. Ayhan, Natural vacuum distillation technique – Part I: Theory and Basics, Intern. J. Energy Res., 28(4) (2004) 355–371.

[13] S. Al-Kharabsheh and D. Y. Goswami, Experimental study of an innovative solar water desalination system utilizing a passive vacuum technique, Solar Energy, 75 (2003) 395–401.

[14] G.A. Bemporad, Basic hydrodynamic aspects of a solar energy based desalination process, Solar Energy, 54 (1995) 125–134.

[15] V.G. Gude and N. Nirmalakhandan, Desalination at low temperatures and low pressures, Desalination, 244 (2009) 239–247.

[16] V.G. Gude, PhD Dissertation, New Mexico State University, Las Cruces, 2007.

[17] V.G. Gude and N. Nirmalakhandan, Combined desalination and solar-assisted air conditioning system, Energy Convers. Manage., 49 (2008) 3326–3330.

[18] V.G. Gude and N. Nirmalakhandan, Desalination using low-grade heat sources, ASCE J. Energy Eng., 134 (2008) 95–101.

[19] Biomass and Alternative Methane Fuels (BAMF) Super ESPC Program Fact sheet, Wastewater Treatment Gas to Energy for Federal Facilities, US department of energy, ORNL 2004-02594/abh, July 2004

[20] F. Banat and N. Jwaied, Economic evaluation of desalination by small scale autonomous solar powered membrane distillation units. Desalination, 220 (2008) 566–573.

[21] American Public Health Association (APHA). Standard Methods for the Examination of Water and Wastewater, 18th ed., Washington, DC, 1992.

[22] H.E.S. Fath, High performance of a simple design, two effect solar distillation unit, Desalination, 107 (1996) 223–233.

Appendix

Energy losses to the ambient can be written as follows [22]:

$$Q_L = Q_c + Q_r + Q_b \tag{A1}$$

Q_L = heat losses from the evaporation chamber (kJ/h-m^2), Q_c = heat losses due to convection (kJ/h-m^2), Q_r = heat losses due to radiation (kJ/h-m^2), Q_b = heat losses through the base (kJ/h-m^2).

$$Q_c = h_{cg} A(T_s - T_g) + h_{cc} A(T_s - T_{co}) \tag{A2}$$

$$h_{cg} = \left(1 - \frac{V_c}{V_e + V_c}\right) h_c \tag{A3}$$

$$h_{cc} = \left(\frac{V_c}{V_e + V_c}\right) h_c \tag{A4}$$

$$h_c = 0.884 \left[\left(T_w - T_g\right) + \frac{\left(P_w - P_g\right)\left(T_w + 273\right)}{268900 - P_w} \right]^{1/3} \tag{A5}$$

$$Q_r = \sigma \varepsilon_w A \left(T_s^4 - T_g^4\right) \tag{A6}$$

$$Q_b = h_b A \left(T_s - T_a\right) \tag{A7}$$

h_{cg} = heat loss coefficient from saline water to glass due to convection (kJ/h-m^2-°C), h_{cc} = heat loss coefficient from saline water to condenser due to convection (kJ/h-m^2-°C), h_c = total heat loss coefficient from saline water due to convection (kJ/h-m^2-°C), h_b = heat loss coefficient through base (kJ/h-m^2-°C).